Kinematics analysis and simulation of a novel metamorphic parallel cutting mechanism

Shenghai Hu[1], Xiulian Liu[1, 2*], Manhui Zhang[1]

[1]*School of Mechanics Engineering, Harbin Engineering University, Harbin 150001, China*

[2]*School of Mechanical Engineering, Heilongjiang University of Science and Technology, Harbin 150027, China*

Received 1 June 2014, www.cmnt.lv

Abstract

Based on the metamorphic mechanisms, we proposed a new type of metamorphic kinematic pair, with which a novel metamorphic parallel cutting mechanism was designed to achieve changing pose and trajectory movement. Using the screw theory and the product of exponentials formula, we constructed a nonlinear system of equations for each configuration framework of the metamorphic parallel cutting mechanism, and the Sylvester resultant elimination method was employed to simplify equations of motion for the mechanism, thereby completing the research about the forward and inverse kinematics solution of the original and sub-configuration framework and verifying the feasibility of this novel mechanism via MATLAB and ADAMS simulation.

Keywords: Metamorphic Mechanism; Screw Theory; Product of Exponentials Formula; Forward and Inverse Kinematics Solution

1 Introduction

The manufacturing of ship products is often accompanied by large-diameter hole cutting and processing on the hull surfaces, which are pieced together with complex surface patches in most cases. And then square groove or bevel preparation of these large size holes are often needed [1-2]. As a critical technical problem in shipbuilding industry, large-diameter-hole and changing-angle bevel structure processing is characterized by high difficulty, low efficiency and low accuracy, etc., and the processing quality of which will directly influence the quality and efficiency of the subsequent industrial processes.

Seamus Gordon, et al., from University of Limerick, designed a high-speed CNC cutting machine realizing spatial movement of the cutting tool along three axial directions. Controlled by computer numerical control programming, the high speed of this cutting device reaches 40m/min [3]. The Omnimat cutting machine developed and produced by Messer, is a high-performance, multi-functional, large CNC cutting machine applicable for high speed and precision cutting of large size flat plate [4]. The model RV-016 cutting robot, developed and produced by Panasonic Corporation, adopts a serial mechanism, and its end infinite rotating cutting gun can perform high speed and precision cutting task on complex surfaces.

In China, many experts and engineering technicians in machinery manufacturing field have made a series of researches on numerical control cutting technology. The multi-functional NC-fair incision machine with a gantry-bridge structure, designed by Ming, et al., can cut large 5000mm × 3000mm work-piece and perform arbitrary plane curve cutting tasks [5]. The cantilever structured CNC large intersecting circle flame cutting machine with five-bar cooperating, designed by Sun, et al., can process a work-piece with a diameter of 4000-8000mm (pipe); and the diameter of the cutting hole lies in a range of 50-550mm, and the bevel angle is between 30° and 40° [6]. Zhang, from Harbin Engineering University, designed a large complex surface cutting mechanism with the end cutting torch being a five-bar metamorphic mechanism to achieve square groove and bevel groove of large diameter hole cutting on complex surfaces; controlled by electric motor, it can perform spatial movements with changing pose and trajectory [7].

Based on the analysis of literatures at home and abroad, we know there are two types of cutting techniques and equipment: one is round hole cutting on a plate with its vertical displacement almost unchanged in the cutting process. And the bevel angle remain unchanged in bevel cutting; the other is CNC pipe-cutting machine, which is applicable for round pipe (whose diameter is less than 1.4m) intersection hole cutting.

The parallel mechanism has the merits of simple high-rigidity structure, high processing speed and accuracy, and is less affected by the inertia, etc. For these advantages over the serial mechanism, it has been widely employed in various processing and manufacturing industries. Furthermore, its end moving platform can many complex spatial motions via multi-axis coordination [8-13]. Studies about metamorphic mechanism starts late, but this mechanism has stimulated the research interests of many scholars for its flexible topology, based on which many tasks can be completed [14-21].

* Corresponding author e-mail: lxl--2002@163.com

According to the principles of metamorphic mechanism, a parallel cutting mechanism was designed to solve the problem of changing pose and trajectory in square groove and bevel groove cutting. Since there are different requirements for the cutting torch motion in the process of cutting different shapes of holes on complex surfaces, we reasonably designed different conFigureuration frameworks of the metamorphic mechanism based on their metamorphic characteristics, which can meet the technology requirements of changing spatial pose and trajectory cutting on large complex surface.

2 Metamorphic Parallel Cutting Mechanism Design

2.1 A NOVEL DESIGN OF SPATIAL METAMORPHIC KINEMATIC PAIR

A conventional spherical pair has three spatial degrees of freedom (DOF). And there are 3 degrees of freedom of rotating between the two components linked by the spherical pair. In actual analysis, the motions of the two components can be simplified as the rotation around the three spatial axes that are perpendicular to each other and also meet the right-hand rule. Therefore, a spatial spherical pair is equivalent to a compound kinematic pair consisting of a Hooke's joint and a revolute pair whose axis is perpendicular to the Hooke's joint axial plane. For a Hooke's joint, the shaft connected with the base is the main shaft, and that connected with the linkage is a counter shaft.

According to the principles of metamorphic mechanism, we designed a slot where the two ends of the counter shaft can slide on the main shaft of Hooke's joint. The counter shaft can be fixed in a certain position as required with a pin; therefore, we can reduce the degree of freedom of the kinematic pair by putting pin into the pinhole located on the revolute pair. Based on the framework before and after metamorphic operation, the novel metamorphic kinematic pair can be classified into four configurations:

(1) The original configuration S_{m3}

Fix the counter shaft in a position perpendicular to the main shaft, and remove the pin on the revolute pair. The kinematic pair has three degrees of freedom and is equivalent to a spatial spherical pair, as shown in Figure. 5(a);

(2) The a-type 2-DOF sub-configuration S^a_{m2}

Fix the counter shaft in a position perpendicular to the main shaft, and put the pin into the pin hole on the revolute pair. Now the kinematic pair has two degrees of freedom and is equivalent to a traditional Hooke's joint, as shown in Figure. 5(b);

(3) The b-type 2-DOF sub-configuration S^b_{m2}

Fix the counter shaft in a co-axial position with the main shaft, and remove the pin on the revolute pair. Now the kinematic pair has two degrees of freedom, as shown in Figure. 5(c);

(4) Sub-configuration S_{ml} with single degree of freedom

Fix the counter shaft in a co-axial position with the main shaft, and remove the pin on the revolute pair. Now the kinematic pair has only one degrees of freedom and is equivalent to a traditional revolute pair, as shown in Figure 1 (d);

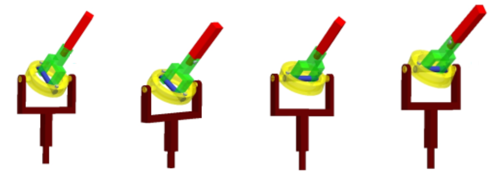

(a) S_{m3} (b) S^a_{m2} (c) S^b_{m2} (d) S_{m1}

FIGURE 1 The Structure of a Novel Metamorphic Kinematic

2.2 THE METAMORPHIC PARALLEL CUTTING MECHANISM'S ORIGINAL CONFIGURATION FRAMEWORK

Based on the above designed metamorphic kinematic pair unit, a limb kinematic chain where we can switch the degree of freedom is constructed. Assign the position of each kinematic pair, and form the metamorphic parallel mechanism using three same limb chains (see Figure 2). The end effectors $M_1M_2M_3$ are connected with the fixed base $B_1B_2B_3$ via the three same kinematic chains $S^a_{m2}S^b_{m2}U$. Under this framework, it is 6-DOF mechanism that can achieve upper and lower bevel cutting. Therefore, it is regarded as the original configuration of the cutting machine. When the mechanical properties of the mechanism are considered, the driving input should be as near as possible to the fixed platform to reduce the influence of inertia and to improve load performance. So we choose three Hooke's joints on the fixed platform as driving input.

2.3 THE NOVEL METAMORPHIC PARALLEL MECHANISM'S SUB-CONFIGURATION FRAMEWORK

Based on the original configuration, the 3-DOF sub-configuration framework of metamorphic parallel mechanism is obtained by transforming the metamorphic kinematic pair S^a_{m2} into S_{m1} framework, and the metamorphic kinematic pair S^b_{m2} into S^a_{m2}. Then the limb chain structure changes after these metamorphic operations. The kinematic pair distribution in the limb chain turns into $S_{m1}S^a_{m2}U$, which means the sub-configuration framework of the metamorphic parallel cutting mechanism is $3S_{m1}S^a_{m2}U$, as shown in Figure 3. With three revolute pairs on the fixed platform chosen as driving inputs, the square groove cutting on the surface can be achieved.

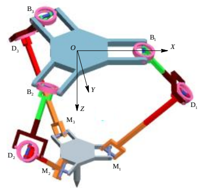

FIGURE 2 The Metamorphic Parallel Mechanism's Original Configuration Framework $3S^a_{m2}S^b_{m2}U$

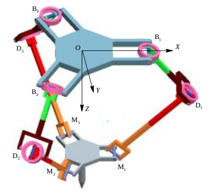

FIGURE 3 3-DOF Sub-configuration Framework $3S_{m1}S^a_{m2}U$

3 The kinematics position analysis of the metamorphic parallel cutting mechanism

3.1 THE ANALYSIS OF THE ORIGINAL CONFIGURATION FORWARD AND INVERSE KINEMATICS SOLUTION

3.1.1 The analysis of original configuration forward kinematics solution

Set the absolute coordinate system $OXYZ$, as shown in Figure 4; the XOY plane is parallel to the plane $B_1B_2B_3$ of the fixed base; axis Z is downward perpendicular to $B_1B_2B_3$; and suppose the origin of coordinates and the geometric centre of $B_1B_2B_3$ overlap. With the structures and parameters of the three limb chains being identical, we assume that: the radius of the circumcircle of $B_1B_2B_3$ is R; the length of $B_iD_i(i=1,2,3)$ is l, and the length of $D_iM_i(i=1,2,3)$ is m. Then suppose the angles of rotation about e_{i1}, e_{i2}, e_{i3}, e_{i4}, e_{i5}, e_{i6} ($i=1\sim3$) in each limb chain are θ_{i1}, θ_{i2}, θ_{i3}, θ_{i4}, θ_{i5} $(i=1\sim3)$ respectively. Let the Hooke's joint of the metamorphic kinematic pair B_i be the driving joint and the rest be driven joint, and $\eta_i(i=1\sim3)$ be the azimuth at point B_i, as shown in Figure 4, where $\eta_1=0^\circ$, $\eta_2=120^\circ$, $\eta_3=\text{-}120^\circ$.

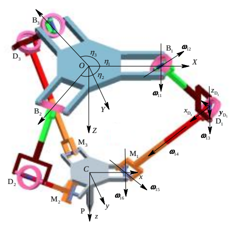

FIGURE 4 The Moving Coordinate System and the Kinematic Screw of the Metamorphic Parallel Cutting Mechanism's Original Configuration Framework

According to rigidity constraint,

$$(M_2-M_1)^T(M_2-M_1)=(M_3-M_1)^T(M_3-M_1) \\ =(M_2-M_3)^T(M_2-M_3)=3r^2 . \tag{1}$$

The coordinates of point M_i in the equation can be obtained through the following methods

$$g_{D_i}(\theta)=e^{\theta_{i1}\hat{\xi}^{\omega}_{i1}}e^{\theta_{i2}\hat{\xi}^{\omega}_{i2}}e^{\theta_{i3}\hat{\xi}^{\omega}_{i3}}g_{D_i}(0), \tag{2}$$

where $e^{\theta\hat{\xi}}=\begin{bmatrix} e^{\theta\hat{e}} & (I-e^{\theta\hat{e}})(e\times v)+\theta e e^T v \\ 0 & 1 \end{bmatrix} \quad (e\neq 0)$,

$\xi=\begin{bmatrix}\omega \\ r\times\omega\end{bmatrix}$, $\hat{\xi}=\begin{bmatrix}\hat{\omega} & r\times\omega \\ 0 & 0\end{bmatrix}$, $\omega=\begin{bmatrix}\omega_1 \\ \omega_2 \\ \omega_3\end{bmatrix}$,

$\hat{\omega}=\begin{bmatrix} 0 & -\omega_3 & \omega_2 \\ \omega_3 & 0 & -\omega_1 \\ -\omega_2 & \omega_1 & 0 \end{bmatrix}$.

$$M_i=R_{D_i}(\theta)M_i^{D_i}+t_{D_i} . \tag{3}$$

Substituting (2) and (3) into (1), we have three equations of $\theta_{i3}(i=1\sim3)$:

$$\begin{cases} L_{11}c\theta_{13}c\theta_{23}+L_{12}s\theta_{13}c\theta_{23}+L_{13}c\theta_{13}s\theta_{23}+L_{14}s\theta_{13}s\theta_{23} \\ +L_{15}c\theta_{13}+L_{16}c\theta_{23}+L_{17}s\theta_{13}+L_{18}s\theta_{23}+L_{19}=0 \\ L_{21}c\theta_{13}c\theta_{33}+L_{22}s\theta_{13}c\theta_{23}+L_{23}c\theta_{13}s\theta_{33}+L_{24}s\theta_{13}s\theta_{33} \\ +L_{25}c\theta_{13}+L_{26}c\theta_{33}+L_{27}s\theta_{13}+L_{28}s\theta_{33}+L_{29}=0 \\ L_{31}c\theta_{23}c\theta_{33}+L_{32}s\theta_{23}c\theta_{23}+L_{33}c\theta_{23}s\theta_{33}+L_{34}s\theta_{23}s\theta_{33} \\ +L_{35}c\theta_{23}+L_{36}c\theta_{33}+L_{37}s\theta_{23}+L_{38}s\theta_{33}+L_{39}=0 \end{cases} , \tag{4}$$

where $L_{mn}(m=1\sim3, n=1\sim9)$ is a polynomial containing $\theta_{i1},\theta_{i2}(i=1\sim3)$.

Based on half-angle formula: $\sin\theta=2\tan(\theta/2)/[1+\tan^2(\theta/2)]$, $\cos\theta=[1-\tan^2(\theta/2))]/[1+\tan^2(\theta/2)]$, supposing $x=\tan(\theta_{13}/2)$, $y=\tan(\theta_{23}/2)$, $z=\tan(\theta_{33}/2)$, and manipulating the above three equations, we have:

$$P_{1y}x^2+P_{2y}x+P_{3y}=0 , \tag{5}$$

$$P_{4x}z^2+P_{5x}z+P_{6x}=0 , \tag{6}$$

$$P_{4y}z^2+P_{5y}z+P_{6y}=0 , \tag{7}$$

where, $P_{1y}=Q_{11}y^2+Q_{13}y+Q_{15}$,
$P_{2y}=Q_{12}y^2+Q_{16}y+Q_{18}$, $P_{3y}=Q_{14}y^2+Q_{17}y+Q_{19}$,
$P_{4x}=Q_{21}x^2+Q_{23}x+Q_{25}$, $P_{5x}=Q_{22}x^2+Q_{26}x+Q_{28}$,
$P_{6x}=Q_{24}x^2+Q_{27}x+Q_{29}$, $P_{4y}=Q_{31}y^2+Q_{33}y+Q_{35}$,
$P_{5y}=Q_{32}y^2+Q_{36}y+Q_{38}$, $P_{6y}=Q_{34}y^2+Q_{37}y+Q_{39}$.

Eliminate the variable z using Sylvester resultant; then regard z and the constant terms as new variables; multiply z with equation (6) and (7), combed with which a matrix is constructed. Since only non-zero solutions are considered, the resultant is zero:

$$\begin{vmatrix} P_{4x} & P_{5x} & P_{6x} & 0 \\ 0 & P_{4x} & P_{5x} & P_{6x} \\ P_{4x} & P_{5x} & P_{6x} & 0 \\ 0 & P_{4x} & P_{5x} & P_{6x} \end{vmatrix} = 0 \cdot \quad (8)$$

Then we have the equation, in which the highest exponent degree of x is not more than 2:

$$F_{1y}x^2 + F_{2y}x + F_{3y} = 0, \quad (9)$$

where $F_{iy}(i = 1 \sim 3)$ are expressions in which the highest exponent degree of y is 2.

Eliminate the variable x using Sylvester resultant; regard x and the constant terms as new variables; multiply x with equation (5) and (10), combed with which a matrix is constructed. Since only non-zero solutions are considered, the resultant is zero:

$$\begin{vmatrix} P_{1y} & P_{2y} & P_{3y} & 0 \\ 0 & P_{1y} & P_{2y} & P_{3y} \\ F_{1y} & F_{2y} & F_{3y} & 0 \\ 0 & F_{1y} & F_{2y} & F_{3y} \end{vmatrix} = 0 . \quad (10)$$

Then we have the equation in which the highest exponent degree of y is not more than 4:

$$K_4 y^4 + K_3 y^3 + K_2 y^2 + K_1 y + K_0 = 0, \quad (11)$$

where $K_l(l = 0 \sim 4)$ is a polynomial containing $\theta_{i1}, \theta_{i2}(i = 1 \sim 3)$. θ_{i1}

Because the driving kinematic pair rotation angles θ_{i1}, θ_{i2} are known quantities, the value of y can be calculated out from equation (11). Substituting the y value into equation (5) and (6), we yield twos sets of values of x and z, and then substituting, which into equation (7) to determine the end values of x and z.

After that, the coordinates of M_1, M_2 and M_3 on the end moving platform can be determined, and then we can further determine the pose of the moving platform in the absolute coordinate system.

3.1.2 The analysis of the original configuration inverse kinematics solution

Supposing that the geometric center of the moving platform is *C*, the cutting gun endpoint is *P*, and the length of the cutting gun is n, we set up the moving coordinate system *Cxyz* of the moving platform $M_1M_2M_3$. The x-axis passes through point M_1; z-axis is perpendicular to the moving platform in an outward direction; and y-axis is determined according to right-hand rule. The analysis of original configuration inverse kinematics solution is to determine the driving kinematic pair rotation angle θ_{i1} and $\theta_{i2}(i = 1 \sim 3)$, based on the known pose of the end moving platform $M_1M_2M_3$. Supposing that the moving coordinate system *Cxyz* is formed by rotating the absolute coordinate system along the X-axis, Y-axis and Z-axis by the angles of γ, β, α respectively, the coordinates of C are (x_C, y_C, z_C), and the coordinates of P is (x_P, y_P, z_P), the pose of centre of mass (PCM) of the end moving platform is represented as:

$$g_C = \begin{bmatrix} R & t_c \\ 0 & 1 \end{bmatrix} = \begin{bmatrix} e^{Z\alpha} e^{Y\beta} e^{X\gamma} & t_c \\ 0 & 1 \end{bmatrix}$$
$$= \begin{bmatrix} c\alpha c\beta & c\alpha s\beta s\gamma - s\alpha c\gamma & c\alpha c\beta c\gamma + s\alpha s\gamma & x_C \\ s\alpha c\beta & s\alpha s\beta s\gamma + c\alpha c\gamma & s\alpha s\beta c\gamma - c\alpha s\gamma & y_C \\ -s\beta & c\beta s\gamma & c\beta c\gamma & z_C \\ 0 & 0 & 0 & 1 \end{bmatrix}. \quad (12)$$

We calculate out the coordinates of M_1, M_2, M_3, P in the moving coordinate system *Cxyz* : $M_1^C(r,0,0)$, $M_2^C(-\frac{1}{2}r, \frac{\sqrt{3}}{2}r, 0)$, $M_3^C(-\frac{1}{2}r, -\frac{\sqrt{3}}{2}r, 0)$, $P^C(0,0,n)$. Therefore, their coordinates in the absolute coordinate system are:

$$M_i = RM_i^C + t_c, \quad (13)$$

$$P = RP^C + t_c. \quad (14)$$

In solving forward kinematics in the above section, we know point M_1, M_2 and M_3 can be represented by θ_{i1}, θ_{i2}, θ_{i3} $(i = 1 \sim 3)$. Based on the corresponding relationship, we have three square matrix equations:

$$\begin{bmatrix} (c\theta_{11}c\theta_{12}\theta_{13} - s\theta_{11}s\theta_{13})m + lc\theta_{11}c\theta_{12} + R \\ -msc\theta_{12}c\theta_{13} - lsc\theta_{12} \\ -(s\theta_{12}c\theta_{13}c\theta_{13} + c\theta_{11}s\theta_{13})m - ls\theta_{11}c\theta_{12} \end{bmatrix} = \begin{bmatrix} rc\alpha c\beta + x_C \\ rs\alpha c\beta + y_C \\ -rs\beta + z_C \end{bmatrix}. \quad (15)$$

$$[p_1 \quad q_1 \quad k_1]^T = [d_1 \quad e_1 \quad f_1]^T, \quad (16)$$

$$[p_2 \quad q_2 \quad k_2]^T = [d_2 \quad e_2 \quad f_2]^T, \quad (17)$$

where $p_1 = -\left[\left(c\theta_{21}c\theta_{22}c\theta_{23} - s\theta_{21}s\theta_{23}\right)m + lc\theta_{21}c\theta_{22} + R\right]/2 + \sqrt{3}\left(ms\theta_{22}c\theta_{23} + ls\theta_{22}\right)/2$,

$$q_1 = \sqrt{3}\left[\left(c\theta_{21}c\theta_{22}c\theta_{23} - s\theta_{21}s\theta_{23}\right)m + lc\theta_{21}c\theta_{22} + R\right]/2 + \left(ms\theta_{22}c\theta_{23} + ls\theta_{22}\right)/2$$

$$k_1 = -\left(s\theta_{21}c\theta_{22}c\theta_{23} + c\theta_{21}s\theta_{23}\right)m - ls\theta_{21}c\theta_{22},$$

$$d_1 = -\gamma c\alpha c\beta/2 + \sqrt{3}\gamma(c\alpha s\beta s\gamma - s\alpha c\gamma)/2 + x_C$$
$$e_1 = -\gamma s\alpha c\beta/2 + \sqrt{3}\gamma(s\alpha s\beta s\gamma + c\alpha c\gamma)/2 + y_C \quad ,$$
$$f_1 = rs\beta/2 + \sqrt{3}rc\beta s\gamma/2 + z_C \quad ,$$
$$f_2 = rs\beta/2 - \sqrt{3}rc\beta s\gamma/2 + z_C$$
$$k_2 = -(s\theta_{31}c\theta_{32}c\theta_{33} + c\theta_{31}s\theta_{33})m - ls\theta_{31}c\theta_{32}$$
$$d_2 = -rc\alpha c\beta/2 - \sqrt{3}r(c\alpha s\beta s\gamma - s\alpha c\gamma)/2 + x_C$$
$$p_2 = -[(c\theta_{31}c\theta_{32}c\theta_{33} - s\theta_{31}s\theta_{33})m + lc\theta_{31}c\theta_{32} + R]/2$$
$$-\sqrt{3}(ms\theta_{32}c\theta_{33} + ls\theta_{32})/2$$
$$q_2 = -\sqrt{3}[(c\theta_{31}c\theta_{32}c\theta_{33} - s\theta_{31}s\theta_{33})m + lc\theta_{31}c\theta_{32} + R]/2$$
$$+(ms\theta_{32}c\theta_{33} + ls\theta_{32})/2$$
$$e_2 = -rs\alpha c\beta/2 - \sqrt{3}r(s\alpha s\beta s\gamma + c\alpha c\gamma)/2 + y_C$$

Based on the coordinates of P in the coordinate system, the coordinates of the centre of mass C of the moving platform can be calculated out. And based on equation (15), (16) and (17), values of θ_{i1}, θ_{i2} and $\theta_{i3}(i=1\sim3)$ can be calculated out, thereby deriving the expressions of θ_{i1} and θ_{i2} in terms of α, β, γ, x_P, y_P, z_P. So the inverse kinematics solution is completed.

3.1.3 A numerical example of forward and inverse kinematics solution

Supposing that the geometric parameters of the original configuration framework of the metamorphic parallel cutting mechanism are: $R=1000$mm, $r=800$mm, $l=1000$mm, $m=1400$mm, $n=200$mm, the coordinates of the cutting gun endpoint P in the absolute coordinate system are (1000,0,1973), and the Euler rotation angles (γ,β,α) are (0°, 30°, 0°), we can calculate out the coordinates of the centre of mass C of the moving platform (900,0,1800). Substituting all these known quantity into the matrix equations of (15), (16) and (17), we obtain the values of input crank rotation angles θ_{i1}, $\theta_{i2}(i=1\sim3)$, and for more detailed calculation results, see Table 1. It can be seen that the input crank rotation angles $(\theta_{11},\theta_{12},\theta_{21},\theta_{22},\theta_{31},\theta_{32})$=(3.445°, 0°, -95.963°, 23.286°, -95.963°, -23.286°) are reasonable solutions of the inverse kinematics.

TABLE 1 Inverse kinematics solution of the metamorphic parallel cutting mechanism's original configuration framework

C (x_c,y_c,z_c) (γ,β,α)	$(\theta_{11}\ \ \theta_{12})$	$(\theta_{21}\ \ \theta_{22})$	$(\theta_{31}\ \ \theta_{32})$
(900,0,1800) (0°,30°, 0°)	(3.445° 0°) (-130.724° 0°) (-49.337°180°) (176.557°180°)	(-95.963°23.286°) (-133.334°23.286°) (95.963° 156.714°) (133.334° 156.714°)	(-95.963°-23.286°) (-133.334°-23.286°) (95.963° -156.714°) (133.334° -156.714°)

Taken $(\theta_{11},\theta_{12},\theta_{21},\theta_{22},\theta_{31},\theta_{32}) = (3.445^\circ, 0^\circ, -95.963^\circ, 23.286^\circ, -95.963^\circ, -23.286^\circ)$ as the input crank rotation angles of the mechanism, we obtain eight sets of forward kinematics solutions by solving the forward kinematics equation of the mechanism. For more detailed calculation results, see Table 2.

It can be seen that the two sets of x and z values calculated out based on the four sets of y values of equation (11) all satisfy equation (7) and thus are all reasonable solutions. Hence, we obtain eight sets of forward kinematics solutions.

TABLE 2 Forward Kinematics Solution of the Metamorphic Parallel Cutting Mechanism's Sub- configuration Framework

No	θ_{13}	θ_{23}	θ_{33}
1	2.5956	3.0572	3.0572
2	1.1422	3.0572	3.0572
3	1.9517+1.2135i	-2.2954+1.0379i	-2.2954+1.0379i
4	-2.1642+0.7489i	-2.2954+1.0379i	-2.2954+1.0379i
5	1.9516-0.2133i	-2.2954-1.0379i	-2.2954-1.0379i
6	-2.1642-0.7484i	-2.2954-1.0379i	-2.2954-1.0379i
7	2.5728	0.6784	0.6784
8	1.8045	0.6784	0.6784

After calculation, the obtained coordinates of M_1, M_2 and M_3 in the absolute coordinate system are shown in Table 3.

TABLE 3 The Coordinates of M_1, M_2 and M_3 in the Absolute Coordinate System

No	M_1			M_2			M_3		
	x_{M_1}	y_{M_1}	z_{M_1}	x_{M2}	y_{M2}	z_{M2}	x_{M3}	y_{M3}	z_{M3}
1	301.79	0	282.205	301.79	0	282.205	301.79	0	282.205
2	-453.439	0	-1418.2	-453.439	0	-1418.2	-453.439	0	-1418.2
3	272.887	0	268.508	272.887	0	268.508	272.887	0	268.508
4	1592.8	0	1400	1592.8	0	1400	1592.8	0	1400

Based on Table 3 and the equation (15), (16) and (17), we can calculate out the coordinates of the geometric center C and the z-y-x Euler angles of the moving platform, see Table 4.

TABLE 4 The coordinates of the geometric centre C and the z-y-x Euler angles of the moving platform

No	C			α	β x_C	γ y_C
	x_C	y_C	z_C			
1	-411.729	0	-79.67	0°	-411.729	0
2	-663.473	0	-646.41	0°	-663.473	0
3	486.443	0	1387.103	0°	486.443	0
4	899.993	0	1800	0°	899.993	0

Since the phase spaces of the first and the third set of solutions will cause interference in the mechanism, and the phase space of the second set is outside the range of maximum rotation angle $\theta_{i3}(i=1\sim3)$, we give all these three sets of solutions up. Errors resulting from using approximate solutions of inverse kinematics to solve the forward kinematics of the mechanism are small between the fourth set of solutions and the inverse kinematics solutions. Figure 5 is the abbreviated drawing of the mechanism pose of the fourth solutions set, and the corresponding model pose is shown in Figure 6.

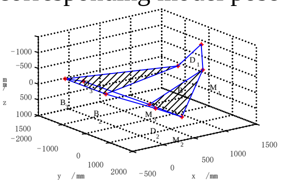

FIGURE 5 Mechanism pose diagram of position positive solutions

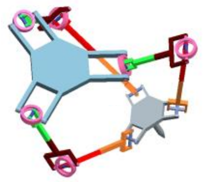

FIGURE 6 Model pose of position positive solutions

3.2 FORWARD AND INVERSE KINEMATIC ANALYSIS OF THE METAMORPHIC PARALLEL CUTTING MECHANISM'S SUB-CONFIGURATION FRAMEWORK

3.2.1 Forward Kinematic Analysis of the Sub-configuration Framework

Figure 7 shows the moving coordinate system and kinematic screw of metamorphic parallel cutting mechanism's the sub-configuration framework. Establish the absolute coordinate system $OXYZ$, and the sub-configuration framework has only 3 degrees of freedom.

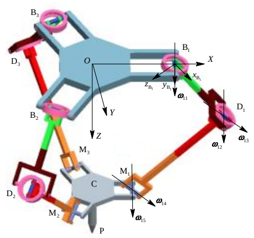

FIGURE 7 Coordinate of motion and twist of sub-configuration

Suppose the angles of rotation about e_{i1}, e_{i2}, e_{i3}, e_{i4}, e_{i5} $(i=1\sim3)$ in each limb chain are θ_{i1}, θ_{i2}, θ_{i3}, θ_{i4}, θ_{i5} $(i=1\sim3)$ respectively. Let metamorphic kinematic pair B_i be the driving joint and the rest be driven joints. Suppose the coordinates of the geometric center C of the moving platform $\mathrm{M_1M_2M_3}$ in the absolute coordinate system are (x_C, y_C, z_C), based on which the coordinates of M_1, M_2, M_3 in the absolute coordinate system are :

$$\begin{cases} \mathrm{M}_1 = \begin{bmatrix} x_C + r & y_C & z_C \end{bmatrix}^{\mathrm{T}} \\ \mathrm{M}_2 = \begin{bmatrix} x_C - r/2 & y_C + \sqrt{3}r/2 & z_C \end{bmatrix}^{\mathrm{T}} \\ \mathrm{M}_3 = \begin{bmatrix} x_C - r/2 & y_C - \sqrt{3}r/2 & z_C \end{bmatrix}^{\mathrm{T}} \end{cases}. \tag{18}$$

To calculate the coordinates of D_i in the absolute coordinate system, let fully expanded limb chain $\mathrm{B_iD_iM_i}$ be the initial phase space, at which the conversion between $\mathrm{B_i}x_{Bi}y_{Bi}z_{Bi}$ and the absolute coordinate system is:

$$g_{\mathrm{B}_i}(\theta) = e^{\theta_{i1}\hat{\xi}_{i1}^{\omega}} g_{\mathrm{B}_i}(0). \tag{19}$$

And the coordinates of D_i in the absolute coordinate system are:

$$\mathrm{D}_i = R_{\mathrm{B}i}\mathrm{D}_i^{\mathrm{B}_i} + t_{\mathrm{B}_i}. \tag{20}$$

According to the rigidity constraint equation $\left|\mathrm{D}_i\mathrm{M}_i\right|^2 = m^2 (i=1\sim3)$, we have the position kinematics equation of the metamorphic parallel mechanism's sub-configuration framework:

$$\begin{cases} (x_c + r - l\cos\theta_{11} - R)^2 + y_c^{\ 2} + (z_c + l\sin\theta_{11})^2 - m^2 = 0 \\ \left[x_c - \frac{1}{2}r + \frac{1}{2}(l\cos\theta_{21} + R)\right]^2 + \left[y_c + \frac{\sqrt{3}}{2}r - \frac{\sqrt{3}}{2}(l\cos\theta_{21} + R)\right]^2 + (z_c + l\sin\theta_{21})^2 - m^2 = 0 \\ \left[x_c - \frac{1}{2}r + \frac{1}{2}(l\cos\theta_{31} + R)\right]^2 + \left[y_c - \frac{\sqrt{3}}{2}r + \frac{\sqrt{3}}{2}(l\cos\theta_{31} + R)\right]^2 + (z_c + l\sin\theta_{31})^2 - m^2 = 0 \end{cases}. \tag{21}$$

Let $a = r - l\cos\theta_{11} - R$, $b = l\sin\theta_{11}$, $e = l\sin\theta_{21}$, $h = l\sin\theta_{31}$, $c = -r/2 + (l\cos\theta_{21} + R)/2$, $d = \sqrt{3}r/2 - \sqrt{3}(l\cos\theta_{21} + R)/2$, $f = -r/2 + (l\cos\theta_{31} + R)/2$, $g = -\sqrt{3}r/2 + \sqrt{3}(l\cos\theta_{31} + R)/2$.

So that the simultaneous equations (21) can be written as:

$$\begin{cases} (x_c + a)^2 + y_c^{\ 2} + (z_c + b)^2 - m^2 = 0 \\ (x_c + c)^2 + (y_c + d)^2 + (z_c + e)^2 - m^2 = 0 \\ (x_c + f)^2 + (y_c + g)^2 + (z_c + h)^2 - m^2 = 0 \end{cases}, \tag{22}$$

which can be simplified to a matrix form:

$$2\begin{bmatrix} a-c & -d & b-e \\ a-f & -g & b-h \end{bmatrix}\begin{bmatrix} x_c \\ y_c \\ z_c \end{bmatrix} = \begin{bmatrix} d^2 - a^2 + c^2 - b^2 + c^2 \\ g^2 - a^2 + f^2 - b^2 + h^2 \end{bmatrix}. \tag{23}$$

Based on equation (23), let z_c represent x_c and y_c, and substitute it into equation (24), thereby deriving the analytic expression of z_c relative to θ_{11}, θ_{21} and θ_{31}. Then x_c and y_c can be calculated out, and the forward kinematics solution is achieved.

3.2.2 Inverse kinematic analysis of the sub-configuration framework

Substituting the half angle formula $\sin\theta = 2\tan(\theta/2)/[1+\tan^2(\theta/2)]$, $\cos\theta = [1-\tan^2(\theta/2)]/[1+\tan^2(\theta/2)]$ into equation (21), we have the expressions of $\tan(\theta_{11}/2)$, $\tan(\theta_{21}/2)$ and $\tan(\theta_{31}/2)$ about x_c, y_c and z_c, thereby obtaining the input crank rotation angles θ_{11}, θ_{21} and θ_{31}. Then the inverse kinematics solution of the sub-configuration framework is achieved.

3.2.3 A numerical example of forward and inverse kinematics solution

Suppose the coordinates of the cutting gun endpoint P are (1000,0,1000), and the coordinates of the moving platform geometric center C are (1000,0,800). Substituting these two known quantities into equation (21), we have the input crank rotation angles θ_{11}, θ_{21} and θ_{31}. See Table 5 for detailed calculation results. The results $\theta_{11} = -156.033^\circ$ and $\theta_{21} = \theta_{31} = -167.665^\circ$ will cause interference or unreasonably distribution of the components in the mechanism, so we give them up. Then supposing the coordinates of the moving platform geometric center C is (-1000,0,200), $\theta_{11} = -159.101^\circ$ and $\theta_{21} = \theta_{31} = -96.178^\circ$ among the results obtained are also unreasonable and are therefore casted.

TABLE 5 Inverse kinematics solution of the metamorphic parallel mechanism's sub-configuration framework

C(x_c, y_c, z_c)	(1000,0,800)	(-1000.0.200)
θ_{11}	23.174°, -156.033°	-159.101°, -146.005°
θ_{21}	-116.654°, 167.665°	-96.178°, 32.956°
θ_{31}	-116.654°, 167.665°	-96.178°, 32.956°

Taken $(\theta_{11}, \theta_{21}, \theta_{31}) = (23.174^\circ, -116.654^\circ, -116.654^\circ)$ in Table.5 as input crank rotation angles, we obtain the forward kinematics solution by solving the forward position equation of the mechanism. See Table 6 for detailed calculation results.

TABLE 6 Forward Kinematics Solution of Metamorphic Parallel Mechanism's Sub-conFigureuration Framework

$(\theta_{11}, \theta_{21}, \theta_{31})$	(23.174°,-116.654°, -116.654°)
C (x_c, y_c, z_c)	(1006.427,0,995.852) (-280.248,0,-429.140)

Obviously, (1006.427,0,995.852) are reasonable solutions; Figure 8 is the corresponding pose of end moving platform at the model mechanism; Figure 9 is the corresponding pose of the model. Taking the inverse kinematics solution results calculated to the thousandth as the input of forward kinematics solution may result in errors between the forward and the inverse kinematics solution results.

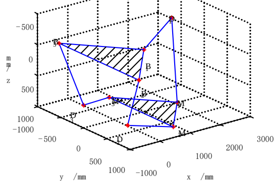

FIGURE 8 Mechanism pose diagram of position positive solutions

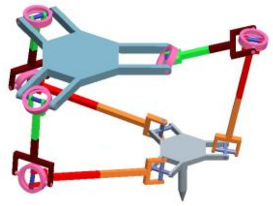

FIGURE 9 Model pose of position positive solutions

4 Study on kinematics simulation of the metamorphic parallel cutting mechanism

4.1 KINEMATICS SIMULATION OF THE METAMORPHIC PARALLEL CUTTING MECHANISM'S METAMORPHIC ORIGINAL CONFIGURATION FRAMEWORK

4.1.1 MATLAB-based kinematics numerical simulation of the original configuration framework

The sub-configuration framework of metamorphic parallel cutting mechanism should be able to perform upper and lower bevel cutting on a surface, which means the end moving platform can move with changing spatial pose and trajectory. Now we take upper bevel cutting as an example, and the space motion requirement for the cutting gun endpoint P are:

$$\begin{cases} x = 1000\sin(2\pi t/2) \\ y = 1000\cos(2\pi t/2) \\ z = -400\sin(2\pi t/2) + 1400 \\ \alpha = 0 \\ \beta = -(\pi/6)\cdot\sin(2\pi t/2) \\ \gamma = (\pi/6)\cdot\cos(2\pi t/2) \end{cases}, \tag{24}$$

where T is a time cycle with the value of 60s.

Set 300 evenly spaced numerical points t from 0 to 60s. Based on the above inverse kinematics equation of metamorphic parallel cutting mechanism's original configuration framework, using Matlab, we calculate out the 300 numerical values of the 6 driving kinematics pairs rotation angles in the original configuration framework. Then draw the curve of driving kinematic pair rotation angles to time based on the numerical values obtained. As shown in Figure 10, compute the derivatives of the analytic expressions of the six input crank rotation angles with respect to t, and obtain 300values of inputs angular velocities. Then draw the angular velocity curve, as shown in Figure 11.

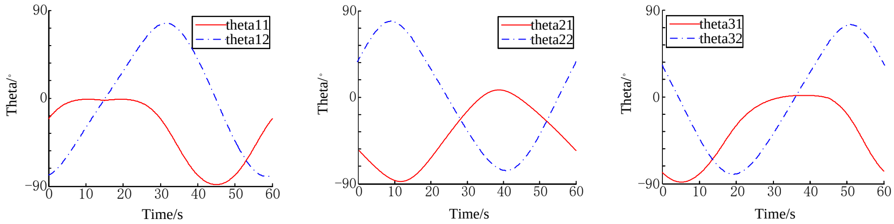

(a) Angle changing curve of the drive pair in the branched chain $B_1D_1M_1$

(b) angle changing curve of drive pair in the branched chain $B_2D_2M_2$

(c) angle changing curve of drive pair in the branched chain $B_3D_3M_3$

FIGURE 10 Input angle curve of source configuration of metamorphic parallel cutting mechanism

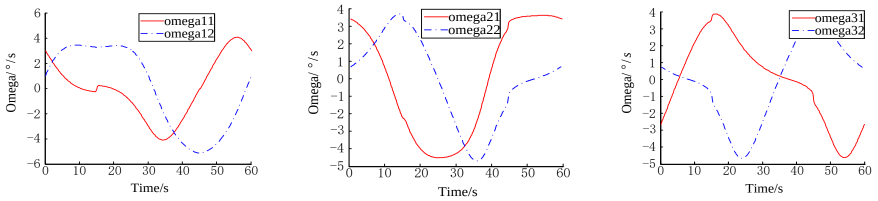

(a) Angular velocity changing curve of drive pair in the branched chain $B_1D_1M_1$

(b) Angular velocity changing curve of drive pair in the branched chain $B_2D_2M_2$

(c) Angular velocity changing curve of drive pair in the branched chain $B_3D_3M_3$

FIGURE 11 Input angular velocity curve of source configuration of metamorphic parallel cutting mechanism

4.1.2 ADAMS-based kinematics simulation of the original configuration framework

Figure 12 shows the simulation model. Add six driving force on the three Hooke's joints; and draw spline curve using the 300 numerical values of driving kinematic pair rotation angles calculated out by MATLAB and add it as driven spline curve to the AKISPL function. Figure 13 is the spline curve of the input crank rotation angle θ_{11}.

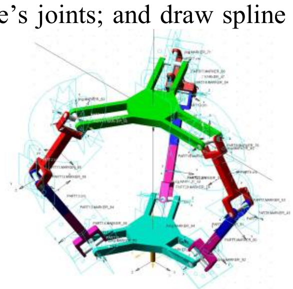

FIGURE 12 Simulation models in ADAMS

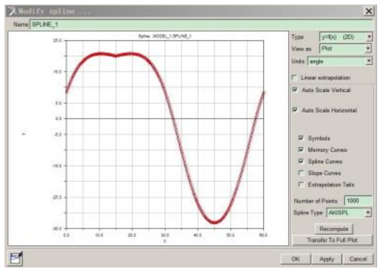

FIGURE 13 The spline curve of input angles

Perform kinematics simulation of the above model by setting the simulation time 60s and the number of time steps 300. And measure the displacement and angle changes of the coordinate system of the end moving platform's center of mass relative to that of the fixed platforms, thereby obtaining the angular displacement and the angular velocity change curves of the end moving platform's center of mass, as shown in Figure 14.

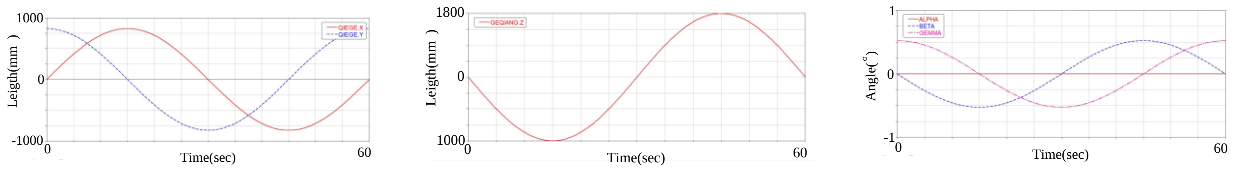

(a) displacement curve on X, Y axis at the end point of cutting gun

(b) displacement curve on Z axis at the end point of cutting gun

(c) angle curve of the end point of cutting gun relative to system coordinate axis

FIGURE 14 Change curves of displacement and angle of the end moving platform's center relative to the static platform

4.1.3 The simulation output analysis

The curve derived from the simulation shows the ADAMS-based simulation output coincides well with the motion characteristics as well as the changing trend of the center of mass of the mechanism end moving platform with initial settings. To find the numerical errors between the simulation output and the theoretical motion characteristics, the simulation values and theoretical values of the each motion parameters at the time of t=0,10,20,30,40,50,60s are collected, thereby obtaining the maximum relative errors. See Table 7 for more detail.

TABLE 7 The Simulation-theoretical Relative Errors of the Mechanism Motion Parameter

Motion Parameters	X(mm)	Y(mm)	Z(mm)	X-Angle(°)	Y-Angle(°)	Z-Angle(°)
Relative Errors	0.0048	0.0059	0.0005	0.006	0.0021	0.0044

Comparing the ADAMS simulation values and theoretical values of motion parameters of the metamorphic parallel cutting mechanism's original configuration framework, as shown in Table 7, we know the maximum relative errors at each time point are all restricted on a level of 0.01. It means the kinematics method adopted in this paper for the study of the metamorphic parallel cutting mechanism's original configuration framework is correct and reasonable, and the bevel cutting on the surface can be achieved via this mechanism.

4.2 KINEMATICS SIMULATION OF THE METAMORPHIC PARALLEL CUTTING MECHANISM'S SUB-CONFIGURATION FRAMEWORK

4.2.1 MATLAB-based kinematics numerical simulation of the sub-configuration framework

The metamorphic parallel cutting mechanism's sub-configuration framework has 3 degrees of freedom, and the motion of the end moving platform is 3D satisfying the requirement of square groove cutting on a surface.

Now we give the specific requirements for trajectory of the cutting gun endpoint:

$$\begin{cases} x = 1000\sin\dfrac{2\pi}{\mathrm{T}}t \\ y = 1000\cos\dfrac{2\pi}{\mathrm{T}}t \\ z = -400\sin\dfrac{2\pi}{\mathrm{T}}t + 1400 \end{cases}, \tag{25}$$

where T is a time cycle with value of 60s.

Set 300 evenly spaced numerical points t from 0 to 60s. Based on the inverse kinematics equation of the sub-configuration framework, using Matlab, we calculate out the input crank rotation angles and angular velocities at the 300 numerical points, and then draw the curve of input rotation angle and angular velocity to time, as shown in Figure 15 and Figure 16.

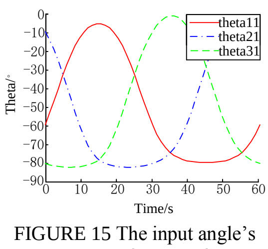

FIGURE 15 The input angle's changing curve of sub configuration

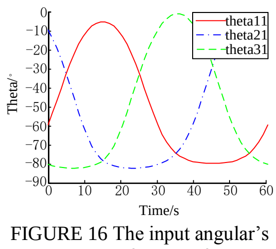

FIGURE 16 The input angular's velocity curve of sub configuration

4.2.2 ADAMS-based kinematics simulation of the sub-configuration framework

The kinematics simulation method applied to the study of the metamorphic parallel cutting mechanism's sub-configuration framework is the same with that applied to the original configuration. And Figure 17 shows the simulation model. Using the same method in section 3.1.2, import the values of the three driving pair rotation angles obtained from MATLAB into ADAMS, and use Spline curve to fit the data points of driving pair rotation angles. Then, set spline-driven pattern for the sub-configuration framework.

Perform kinematics simulation of the above model by setting the simulation time 60s and the number of time steps 300. And measure the displacement and angle changes of the coordinate system of the center of mass of the end moving platform relative to that of the fixed platforms, thereby obtaining the angular displacement and the angular velocity change curves of the center of mass of the end moving platform, as shown in Figure 18.

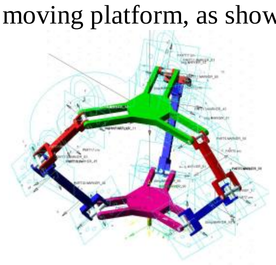

FIGURE 17 The ADAMS Simulation Model

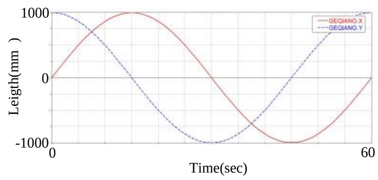

(a) X, Y axis displacement curve of cutting gun end point

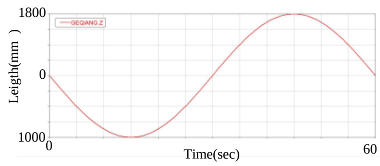

(b) Z axis displacement curve of cutting gun end point

FIGURE 18 Each axis displacement curve of the end moving platform's centroid

4.2.3 The simulation output analysis

The analysing method is the same as that applied to the original configuration framework. Similarly, the ADAMS simulation values and theoretical values (motion values of the end moving platform's center of mass in the mechanism with initial settings) of the each motion parameters at the time of t=0,10,20,30,40,50,60s are collected, thereby obtaining the maximum relative errors as shown in Table 8.

TABLE 8 The Simulation-theoretical Relative Errors of the Mechanism's Motion Parameters

Motion Parameters	**X(mm)**	**Y(mm)**	**Z(mm)**
Relative Errors	0.0028	0.0045	0.0013

Comparing the ADAMS simulation value and theoretical value (the mechanism with initial settings) of the motion parameters of the metamorphic parallel cutting mechanism's sub-configuration framework, as shown in Table 8, we know the maximum relative errors at each time point are all restricted to a level of 0.01. It means the kinematics method adopted in this paper for the study of sub-configuration framework is correct and reasonable, and the bevel cutting on the surface can be achieved via this mechanism.

5 Conclusions

(1) Based on the traditional spherical pair, a novel metamorphic kinematic pair with four different frameworks was designed according to the principles of metamorphic mechanism. And then we devised a metamorphic parallel cutting mechanism structure using this kinematic pair.

(2) We analysed the forward and the inverse kinematics solution for the original and the sub-configuration of the metamorphic parallel cutting mechanism respectively, and made numerical example verification using MATLAB. Finally, the ADAMS simulation showed that this novel metamorphic parallel cutting mechanism is capable of square groove and bevel cutting on complex surfaces satisfying the technical requirements of changing spatial pose and trajectory cutting on complex large-size surfaces.

Acknowledgements

This work is supported by National Natural Science Foundation of China (51175099).

References

[1] Jinli Lv 2009 Design and Simulation on Series-parallel Mechanisms of cutting machines for complex surface. Harbin Engineering University 1-3
[2] Zongyi Wang, Shenghai Hu, Shijun Zhao 2003 Design of big intersecting circle flame cutting machine *Journal of Harbin Engineering University* **24**(3) 258-62
[3] Xiaodong Zhang 2012 *Design and dynamic characteristics study on metamorphic mechanisms of cutting machines for complex surface* Harbin Engineering University 1-3
[4] Seamus Gordon, Hillery M T 2005 Development of a high-speed CNC cutting machine using linear motors *Journal of Materials Processing Technology* **166** 321-9
[5] http://www.messercs.cn/pt/asiapacific/systems/machines/metalmaster/
[6] Xingzu Ming, Jinhua Liu 2005 Design of large-scale NC-fair incision machine with multi-functions *Modern Manufacturing engineering* 107-9
[7] Meina Sun, Yongchun Zheng, Zhenrong Gang 2007 Design of CNC.big intersecting circle flame cutting machine *Machinery Design & Manufacture* (10) 139-40
[8] Kumar Vijay 1990 Characterization of Workspaces of Parallel Manipulators *Mechanism Synthesis and Analysis* (25) 321-9
[9] Boudreau R, Gosselin V 1999 The Systhesis of Planar Parallel Manipulators with a Genetic Algorithm *ASME Journal of Mechanical Design* **12**(4) 533-7
[10] Feng Gao 2005 Reflection on the current status and development strategy of mechanism research *Chinese Journal of mechanical engineering* **41**(8) 3-17
[11] Shu Zhang, Heisel U 2003 *Parallel Kinematics Machine Tool* 1st ed. Beijing: Machinery Industry Press, China
[12] Bhattacharya S, Hatwal H, Ghosh A 1995 On the Optimum Design of a Stewart Platform Type Parallel Manipulators *Robotica,* **13** 133-40
[13] Yang Zhao 2014 Study on Predictive Control for Trajectory Tracking of Robotic Manipulator *Journal of Engineering Science and Technology Review* **7**(1) 45-51
[14] Shu Xu, etc. 2014 Local fractional Laplace variational iteration method for non-homogeneous heat equations arising in fractal heat flow *Mathematical Problems in Engineering* **2014** 1-10
[15] Dai J S, Zhang Q 2000 Metamorphic mechanisms and their configuration models *Scientific Journal of Mechanical Engineering the Scientific Journal of Chinese Mechanical Engineering Society* **13** 212-8
[16] Zongh Guo, Lvzhong Ma, Qizhi Yang 2005 Topological type analysis of the variable freedom mechanism based on the metamorphic principle *China Mechanical Engineering* **16** 1-3
[17] Zhang P, Dai J S 2009 Metamorphic techniques and geometric reconfiguration principles *Proceedings of the 2009 ASME/IFToMM International Conference on Reconfigurable Mechanisms and Robots* 32-40
[18] Shujun Li, Dai J S 2011 Topological representation of planar mechanisms based on Assur group elements *Journal of mechanical engineering* **47** 8-12
[19] Xianjin Wang, Yang Zhao, Xiaojun Yang 2014 Local fractional variational iteration method for inhomogeneous Helmholtz equation within local fractional derivative operator M*athematical Problems in Engineering* **2014** 1-10
[20] Dai J S, Jones J R 1999 Mobility in metamorphic mechanism of foldable/ereetable kinds *Transaction of the ASME, Journal of Mechanical Design* **121**(3) 375-82
[21] Dai J S, Zhang Q X 2000 Metamorphic mechanism and their configuration models *Chinese Journal of Mechanical Engineering (English Edition)* **13**(3) 212-8

Authors

Shenghai Hu, born on October 5, 1954, China

Current position, grades: Professor, College of mechanical engineering of Harbin Engineering University, a member of the Institute of China shipbuilding Surface weapon Society. He is engaged in the study of naval gun weapon system, NC machining technology, mechanical design theory and so on. He has won first prize of progress of science and technology of Heilongjiang Province, and has awarded the second prize of state scientific and technological progress.
Publications: edited three books and published more than 40 Academic papers.

Xiulian Liu, born on March 19, 1979, China

Current position, grades: lecturer, ph.D. degree in mechanical design from Liaoning technical university, China in 2005.
Scientific interests: the application of variable topology mechanism, NC machining technology.

Manhui Zhang, born on May 24, 1991, China

Current position, grades: ph. degree in mechanical design from Harbin Engineering University, China in 2012.
Scientific interests: the application of variable topology mechanism, NC machining technology.